

Influence and modelling of view angles and microrelief on surface temperature measurements of bare agricultural soils

Michel Verbrugghe^{a,*}, Jerzy Cierniewski^b

^a INRA, Bioclimatologie, Site Agroparc 84914, Avignon cedex 9, France

^b Adam Mickiewicz University, Institute of Physical Geography, Fredy 10, 061-701 Poznan, Poland

Received 25 November 1996; accepted 15 February 1998

Abstract

The exploitation of remote sensing instruments with large fields of view necessarily implies the analysis of instruments acquired over a wide variety of viewing geometries. The purpose of this study is to underline the effects of view angles and microrelief on the directional surface temperature measurements of cultivated bare soils. A campaign of measurements was carried out at Poznan (Poland) in April 1995. The directional temperatures were measured on a furrowed sandy soil. The measurements were acquired at ground level with a radiothermometer in the 8–14 μm band. The radiothermometer was fixed on a special goniometric support 2.1 m above the soil surface and was directed at the soil with view zenith angles varying from -60° to $+60^\circ$ by steps of 10° . The data were collected for solar zenith angles ranging from 40.2° to 62.3° . In the experiment, for a given sun position, the difference between oblique and nadir measurements could reach 6°C . A model aimed at explaining the variations of the surface temperature measurements of furrowed soil in relation to its viewing conditions is presented. This model requires the precise soil microrelief geometry configuration, the illumination and viewing conditions of the surface and the radiative temperatures of the shaded and sunlit soil facets. The results show a good correlation between the predicted and the measured data. This type of modelling can be used to correct radiative temperature measurements of soils from view angles and soil microrelief geometry effects. © 1998 Elsevier Science B.V. All rights reserved.

Keywords: agricultural soil; surface temperature; view angle; geometrical modelling

1. Introduction

The radiative temperature of the soil surface is an important physical parameter to monitor, because it partly controls the exchanges of sensible and latent heat, as well as the thermal infrared radiative fluxes between the surface and the atmosphere. In particular, it makes it possible to use ancillary me-

teorological data to estimate the latent heat flux and water budgets of agricultural surfaces (Huband and Monteith, 1966; Jackson et al., 1977; Price, 1982; Seguin and Itier, 1983; Kustas et al., 1990).

The surface temperature depends not only on the thermal irradiance, slope, emissivity and thermal conductivity of the soil, but also on the microrelief configuration and viewing geometry. These latter two aspects are presented in this study. The corrections of radiative temperature measurements from the view angle effects are particularly useful in analysing data

*Corresponding author. Fax: (33) 04 90 316420; E-mail: verbruge@avignon.inra.fr

from satellite sensors which are capable of off-nadir viewing, as the result of their wide field of view, such as the AVHRR instrument of the NOAA satellites. They are also necessary for data obtained from bi-angular sensors such as the ATSR radiometer of the European Remote Sensing Satellite (ERS1). In the same way, it is also necessary to know the effects of the view angle to interpret thermal data acquired at ground or aircraft level with multiangle radiometers such as the DAIS or imaging spectrometers such as MIVIS or TIMS.

This paper analyses the thermal directional radiances in relation with the microrelief defined as the microtopography resulting of farming work on a sandy soil. This sandy soil was chosen because it represents 26.8% of agricultural soils in Poland and also because its texture reduces the influence of surface irregularities of aggregates and clods found on other soils and which can disturb the effects of the microrelief on the thermal directional radiances distribution. The effects of viewing geometry on the

surface temperature measurements are discussed using experimental data acquired at ground level with a radiothermometer in the 8–14 μm band. The results are then compared to the outputs of a geometrical model which computes the composite temperature of the targets for each sun and view geometry.

2. The experiment

The experiment was conducted near Poznan (52.46°N, 16.94°E) on 23 April 1995, under clear sky conditions, on a horizontal sandy surface over which an artificial microrelief constituted by furrows was created. The spatial variability of the soil microrelief configuration was therefore considered as being negligible. The microrelief was constituted by a succession of parallel trihedrons oriented in the north–south direction (Fig. 1). This soil surface geometry simulated the form of a furrowed soil surface, such as we can find in agricultural areas (potatoes, cotton etc.). The size of the total furrowed area was a

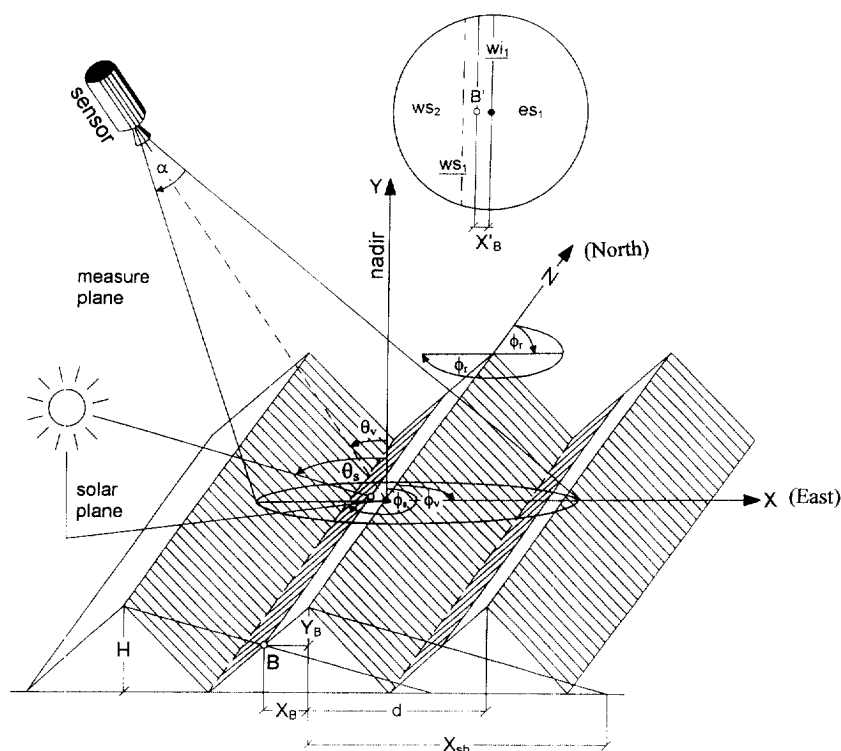


Fig. 1. Geometrical configurations and parameters of soil roughness and view and sun angles.

square of about $3 \times 3 \text{ m}^2$, much larger than the target taken into account by the sensor in every view angle situation. The height of the furrows was 0.08 m, and the distance between two adjoining summits was 0.17 m, the slopes on both sides of the furrows were the same. The dimensions of the trihedrons were determined so that the sensor took into account a base area in vertical view, representative of the whole experimental surface, this latter being constituted by a juxtaposition of similar base areas.

The radiometer was fixed on a goniometric support 2.10 m above the soil surface and described a 180° arc of a circle in a fixed azimuth: the west–east vertical plane, which was perpendicular to the furrows. The measurements were carried out turning, with 10° increments of view zenith angles, from -60° to $+60^\circ$. The negative angles corresponded to forward-scattering directions of observation (the radiometer faces into the sun), the positive angles corresponded to backward-scattering directions (the radiometer faces away from the sun). In the vertical view, the base area viewed by the radiometer was a 0.085 m diameter circle with an area of 227 cm^2 . With a 60° view zenith angle, the target was constituted, in the solar principal plane, by two half ellipses whose radii were 0.16 m and 0.18 m. These two half ellipses had an area of 213.6 cm^2 and 244.3 cm^2 .

The measurements were taken, throughout the day for solar zenith and azimuth angles varying respectively from 40.2° to 62.3° and from 178° to 253° with regard to the geographic north. For each position of the sun reference temperatures were measured at nadir viewing at the beginning, middle and end of each sequence of measurements, the latter being defined by the set of data acquired for all the view angles for each sun position. The duration of each sequence was about 3 min; for each sequence, a reference temperature was determined by the mean value of the three nadir measurements.

The radiative temperatures of sunlit and shaded surfaces of each slope of the furrow were measured separately and manually, at the end of each sequence with the same radiometer and field of view. During these measurements, the radiometer was directed perpendicularly to the plane of the sunlit and shaded surfaces of the two slopes of the furrow. The radiometer was oriented on the centre of the shaded and sunlit facets of the slopes

at a distance of about 0.3 m, the target being a circle whose radius was 0.035 m.

The thermal directional radiance was measured in the $8\text{--}14 \text{ }\mu\text{m}$ spectral band with an EVEREST infrared radiometer model 112ALCS. The resolution of this radiometer is 0.01°C , and its accuracy $\pm 0.5^\circ\text{C}$.

3. The modelling procedure

The angular variation of the thermal emissivity of soil is not thoroughly known but some experimental approaches have shown that the variation of the relative angular emissivity of sand was negligible for view zenith angles between 0 and 50° and about 1% lower for 60° (Becker, 1981; Stoll et al., 1991). In a first approximation, we assumed that the directional emissivity effects of the sandy experimental surface were negligible. Second, we considered that the soil surface temperatures were stable during each sequence of measurements, the differences of temperature between the nadir measurements at the beginning and at the end of each sequence being lower than 0.5°C . The modelling procedure was based on the assumption that the variations in the measured surface temperatures of the soil target could be explained mainly by the precise geometrical configuration of the microrelief, the illumination and viewing conditions of the surface, the fraction of area of the shaded and sunlit facets and their radiative temperatures.

3.1. Geometrical modelling of the fractional sunlit and shaded areas

The geometrical modelling presented here is derived from a previous model relative to a flat ground covered by pebbles (Cierniewski and Verbrugghe, 1994).

The micro-slopes of the experimental furrowed soil are shaded when $\theta_s > \arctan(d/2H)$. The position of the border point B (X_B, Y_B) (Fig. 1), describing the position of the line between the sunlit and shaded fragments of the soil slopes in the vertical projection, perpendicular to the direction of the furrows, was found as the intersection point between the sunbeam and the section of the soil slope in this projection as:

for $\phi_s < 180^\circ$

$$X_B = d^2 / (2X_{sh} + d) \text{ and} \quad (1)$$

$$Y_B = -2HX_{sh}/d \text{ when } X_B < d/2,$$

$$\text{or } Y_B = 2HX_{sh}/d - 2H \text{ when } X_B > d/2,$$

for $\phi_s \geq 180^\circ$

$$X_B = -d^2 / (2X_{sh} + d) \text{ and} \quad (2)$$

$$Y_B = 2HX_{sh}/d \text{ when } X_B > -d/2,$$

$$\text{or } Y_B = -2HX_{sh}/d + 2H \text{ when } X_B < -d/2,$$

where: $X_{sh} = H / \tan(90 - \theta_s) |\cos(\phi_r - \phi_s)|$ and H = height of the furrows (m), d = distance between two adjoining summits (m), θ_s = solar zenith angle (degrees), ϕ_s = solar azimuth angle (degrees), ϕ_r = azimuth orientation of the furrows.

For the furrows oriented in the N–S direction $\phi_r = 90^\circ$ when $\phi_s < 180^\circ$, and $\phi_r = 270^\circ$ when $\phi_s \geq 180^\circ$. The position of the border point B (X'_B, Y'_B) inside the radiometer field of view (FOV) viewed at a given view zenith angle (θ_v) is described as:

$$X'_B = X_B \cos \theta_v - Y_B \sin \theta_v \quad (3)$$

$$Y'_B = X_B \sin \theta_v - Y_B \cos \theta_v$$

Multiplying the X'_B by the fraction $h_r / (h_r - Y'_B)$, where h_r = distance of the radiometer to the summit top, we obtain the proper position of the B' point (position of B in off-nadir viewing) taking into account the conical character of radiometer viewing.

The fraction of shaded and sunlit fragments of the west and the east slopes were calculated as segments of the radiometer FOV circle.

3.2. Composite soil surface temperature modelling

If we consider the radiative energy balance of the soil surface, the composite temperature of the target viewed by the radiometer is a function of the soil sunlit and shaded facet temperatures and of their respective fractional area. This can be expressed by the equation:

$$\epsilon \sigma T_c^4 = f_{sw} \epsilon \sigma T_{sw}^4 + f_{iw} \epsilon \sigma T_{iw}^4 + f_{se} \epsilon \sigma T_{se}^4 + f_{ie} \epsilon \sigma T_{ie}^4 + (1 - \epsilon) I^* \quad (4)$$

with: $f_{sw} + f_{iw} + f_{se} + f_{ie} = 1$,

where ϵ = emissivity of the soil surface, σ = the Stefan–Boltzmann constant ($5.67 \times 10^{-8} \text{ W m}^{-2} \text{ K}^{-4}$), T_c = composite temperature of the soil surface (K), f_{sw} and f_{iw} = calculated fractions of shaded and sunlit facets on the west slope, T_{sw} and T_{iw} = measured temperatures of shaded and sunlit facets on the west slope, f_{se} and f_{ie} = calculated fractions of shaded and sunlit facets on the east slope, T_{se} and T_{ie} = measured temperatures of shaded and sunlit facets on the east slope, and I^* = thermal irradiance of the surrounding received by the surface (W/m^2).

If the emissivity of the sandy soil surface is assumed to be between 0.95 and 0.98 (Stoll et al., 1991) then the term of the thermal reflected irradiance of Eq. 4 for the purpose of this study can be neglected (Kustas et al., 1990).

On the other hand, if we consider only the 8–14 μm band and not the entire spectrum as in Planck's radiation law, the error on energy calculation is also negligible. In fact, the ratio of the irradiance over the whole spectrum to the irradiance over the 8–14 μm band changes to the order of 4% when the temperature varies from 30°C to 70°C (Singh, 1985).

The Eq. 4 can then take the simplified form:

$$T_c^4 = f_{sw} T_{sw}^4 + f_{iw} T_{iw}^4 + f_{se} T_{se}^4 + f_{ie} T_{ie}^4 \quad (5)$$

4. Results

The results of the soil directional radiative temperatures are presented for each sequence in terms of differences between the off-nadir temperatures and the mean value of the three nadir temperatures of the sequence. This methodology for measuring the relative value of the soil temperature also avoids field calibrations which are generally necessary with this type of sensor. In ground measurement conditions, a derivation of the calibration coefficient of the radiothermometers is generally observed in relation with the variations of the external conditions of measurements (Verbrugghe and Guyot, 1992).

4.1. Field measurements

The view and sun angle effects on the directional infrared temperature of the soil are illustrated in Fig. 2. The results show a large dissymmetry between the forward-scattering and the back-scattering view angles. The differences of temperatures are rel-

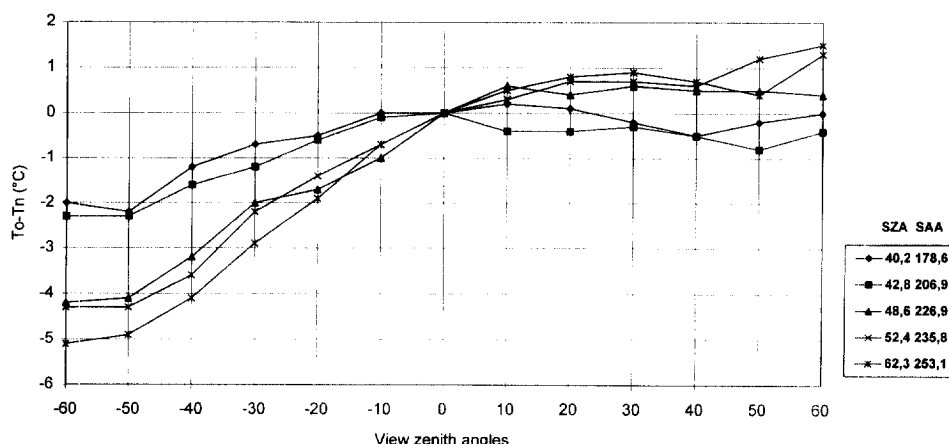


Fig. 2. Variations of the difference between temperature measured in off-nadir viewing (T_o) and temperature measured in nadir viewing (T_n) for different solar zenith angles (SZA) and solar azimuth angles (SAA). Negative angles correspond to forward-scattering observations and positive angles to back-scattering observations.

atively small ($\pm 1^\circ\text{C}$) for all the view and sun angles in back-scattering viewing contrary to forward-scattering viewing, where the differences can reach 5°C . The difference between off-nadir and nadir temperatures increases with the view and sun zenith angles. The smallest differences (-2° in forward-scattering viewing to $+1.5^\circ$ in backward-scattering viewing) are measured when the sun azimuth angle approaches the azimuth angle of the furrows (SAA = 178.6°). The differences of temperatures increase from -5°C in forward-scattering direction to 1.3°C when the solar plane becomes perpendicular (SAA = 253.1°) to the soil facet planes. We can note that the small variations of sun zenith angles induce large discrepancies between oblique and nadir radiative temperatures. These angular variations are similar to those observed over a ploughed bare soil surface (Lagouarde et al., 1995).

4.2. Modelling results

The results of the modelling were compared with the experimental data (Fig. 3). For all the azimuthal and zenithal sun positions, the measured soil temperature curves are similar to those predicted by the modelling. The regression analysis performed between all the measured and predicted data yields good correlation coefficients; the coefficient of determination is 0.949 and the root mean square error 0.96°C (Fig. 4).

On the basis of this modelling, in order to show the influence of the soil microrelief, the effects of furrow orientations and view angles on soil radiative temperatures were simulated. This simulation was performed with the same general experimental conditions presented previously for one sun position (SZA = 62.3° and SAA = 253°). For this situation, the areas of the illuminated and shaded facets of the western and eastern soil slopes were calculated for azimuthal positions of the furrows changing from 165° to 345° by steps of 15° . A coefficient of proportionality of energy was then calculated taking into account the sunbeam incidence angle on the illuminated eastern and western soil slope fragments for the different orientations of the furrows. This coefficient was then applied to the measured temperatures relative to position of the sun mentioned above, to calculate the temperatures of the illuminated soil facets in the other furrow orientation situations. In this simulation, the temperatures of the shaded facets were considered to be constant for each simulated orientation of the furrows and equal to the measured temperature. In the last step, the distribution of the soil radiative temperatures was calculated using Eq. 5. The results of this simulation are illustrated by Fig. 5 which shows the magnitude, at a given instant, of the variations of the soil radiative temperatures depending on the view angles and of azimuth of the furrows. In this simulation, the variation of temperature between forward- and back-scattering directions

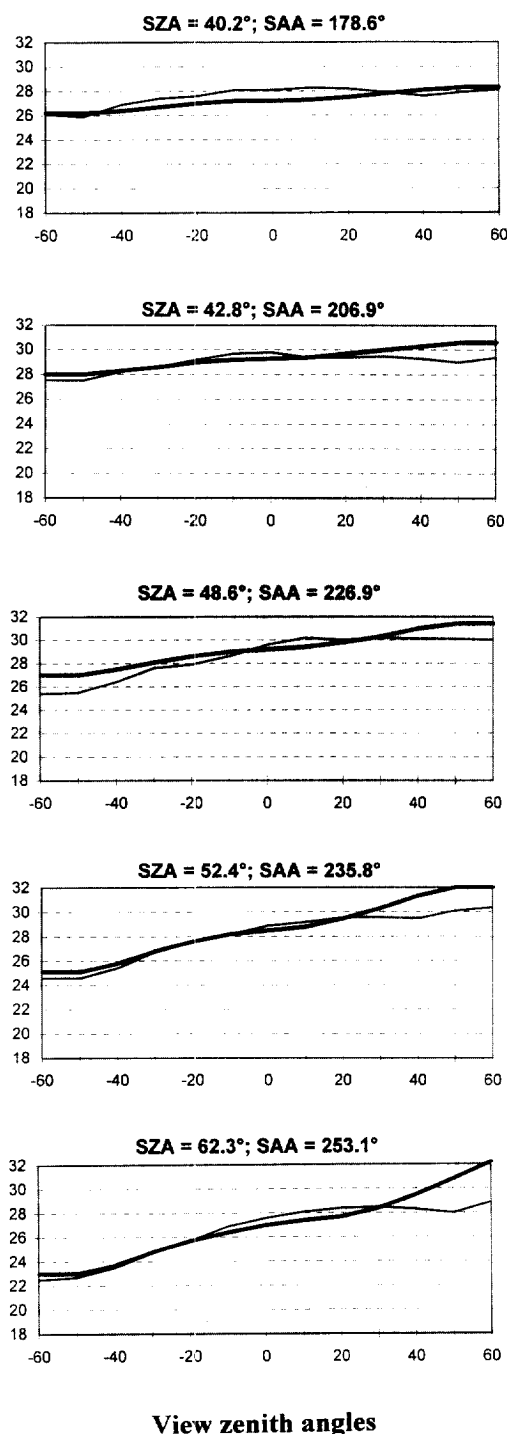


Fig. 3. Relationship between the temperatures predicted by the model (heavy type line) and the measured temperatures (normal type line) for different solar zenith angles (SZA) and solar azimuth angles (SAA).

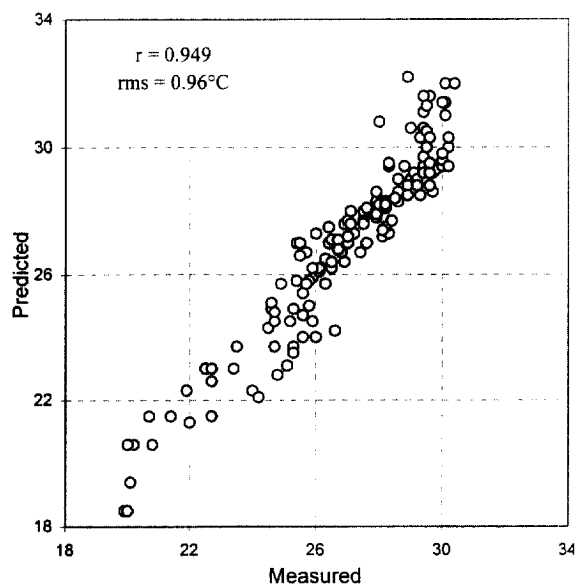


Fig. 4. Relationship between predicted and measured radiative soil temperatures for the different solar zenith angles (SZA) and solar azimuth angles (SAA).

can reach 9°C when the furrows are perpendicular to the solar plane.

In this way, in the experimental conditions described above, the classical calculation of the sensible heat flux, determined from the difference between the soil surface temperature and the air temperature and the aerodynamic resistance, showed large errors in evaluation connected with view angle effects. While the relative error in the sensible heat flux was quite small (overevaluation of 20%) in back-scattering directions, in forward-scattering directions we obtained an underevaluation which could reach 140% for a view angle of -60° and a sun zenith angle of 62.3° . These results showed that the effects of view angles on this type of microrelief could considerably modify the values of the sensible heat flux and consequently the estimation of the soil energy budget.

5. Conclusions

The results underline how the effects of bare soil microrelief created by farming activities on horizontal surface and the angular observation geometries are significant in analysing soil radiative tempera-

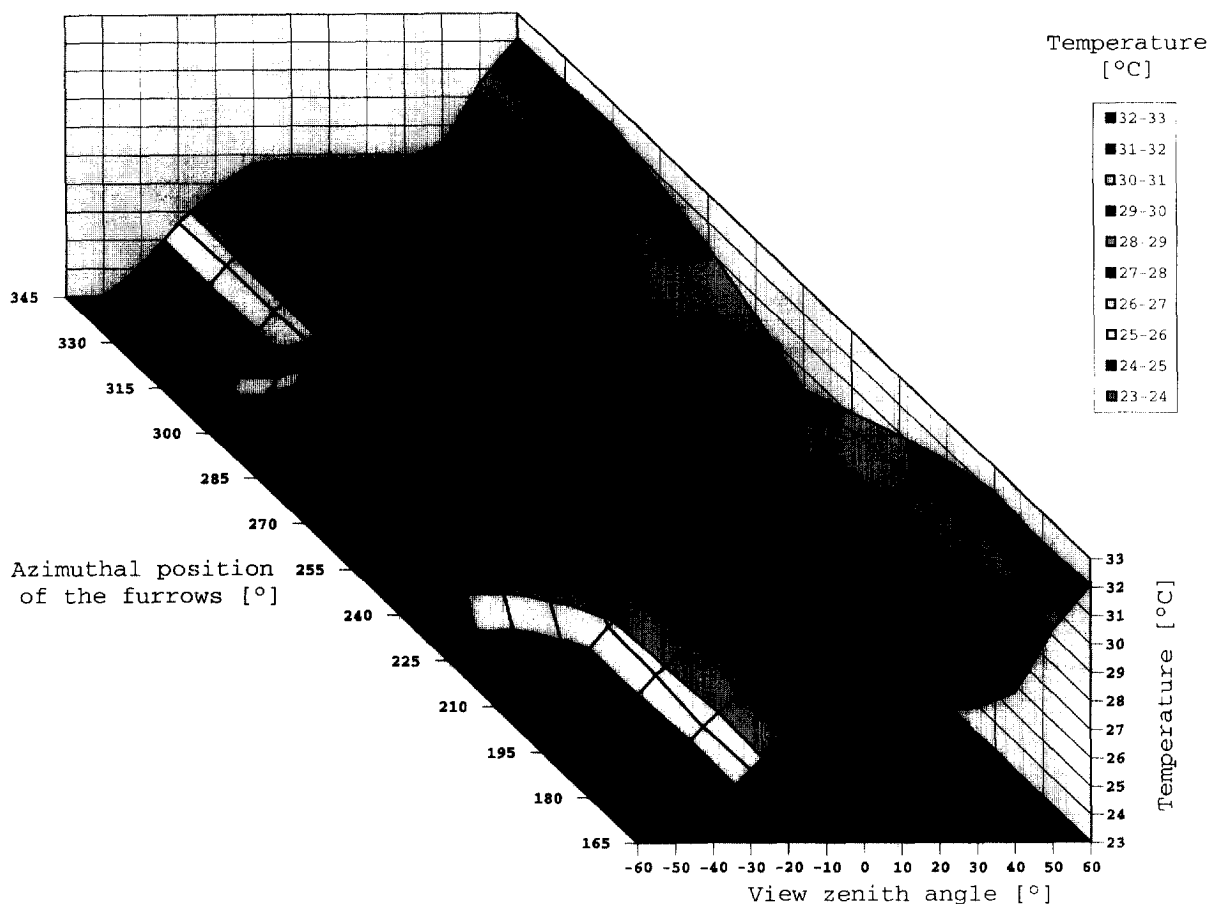


Fig. 5. Simulation of the variations of the soil radiative temperatures versus the view angles and the furrow orientations.

ture measurements. Without the corrections relative to the microrelief and to the view angle effects, the remote sensing thermal data acquired from ground to satellite levels in oblique viewing can introduce large errors in radiative temperature measurements and consequently on the evaluation of the soil energy budget.

Microrelief geometry appears to be a deciding factor in radiative temperature distribution. A simple model taking into account the precise soil microrelief geometry and the radiative temperatures of all the shaded and illuminated facets composing the targets makes it possible to correct these view and microrelief effects. This type of correction of thermal remote sensing data has to be tested on other types of agricultural surfaces.

References

- Becker, F., 1981. Angular reflectivity and emissivity of natural media in the thermal infrared band. *Proc. 1st Int. Colloq. Spectral Signatures of Objects in Remote Sensing*, Avignon, 8–11 Sept. 1981, pp. 57–72.
- Cierniewski, J., Verbrugghe, M., 1994. A geometrical model of soil bidirectional reflectance in the visible and near-infrared range. *Proc. 6th Int. Symp. Physical Measurements and Signature in Remote Sensing*, Val d'Isère, 17–21 Jan. 1994, pp. 635–642.
- Huband, N.D.S., Monteith, J.L., 1966. Radiative surface temperature and energy balance of a wheat canopy, I. Comparison of radiative and aerodynamic canopy temperature. *Boundary Layer Meteorol.* 36, 1–17.
- Jackson, R.D., Reginato, R.J., Idso, S.B., 1977. Wheat canopy temperature: a practical tool for evaluating water requirements. *Water Resour. Res.* 13, 651–656.
- Kustas, W.P., Choudury, B.J., Inoue, Y., Pinter, P.J., Moran, M.S., Jackson, R.D., Reginato, R.J., 1990. Ground and aircraft

- infrared observations over a partially vegetated area. *Int. J. Remote Sensing* 11, 409–427.
- Lagouarde, J.P., Kerr, Y.H., Brunet, Y., 1995. An experimental study of angular effects on surface temperature for various plant canopies and bare soils. *Agric. For. Meteorol.* 77, 167–190.
- Price, J.C., 1982. Estimation of regional scale evaporation through analysis of satellite thermal infrared data. *IEEE Trans. Geosci. Remote Sensing* GE-20, 286–292.
- Seguin, B., Itier, B., 1983. Using midday surface temperature to estimate daily evaporation from satellite thermal IR data. *Int. J. Remote Sensing* 4, 371–383.
- Singh, S.M., 1985. Remarks on the use of a Stefan–Boltzmann type relation for estimating surface temperatures. *Int. J. Remote Sensing* 6, 741–747.
- Stoll, M.P., Nerry, J., Labed, N., Kologo, N., 1991. Approche expérimentale des problèmes d'émissivité et température de surface en télédétection infrarouge thermique. *Proc. 5th Int. Colloq. Physical Measurements and Signatures in Remote Sensing*, Courchevel, 14–18 January 1991, pp. 349–344.
- Verbrugghe, M., Guyot, G., 1992. Note sur l'étalonnage de radiothermomètres infrarouges portables. *Agronomie* 12, 79–83.